Hybrid towers for offshore wind energy converters

Peter Schaumann & Christian Keindorf
ForWind – Center for Wind Energy Research
Institute for Steel Construction, Leibniz University Hannover
Hannover, Germany

ABSTRACT

A new kind of tower construction, calling hybrid tower, is developed for offshore wind energy converters. The tower sections consist of two steel shells which are bonded together with a core material. The core between the inner an outer steel face increases the stability of the shells. In comparison with linear buckling analyses the validity of a laminate composite shell theory was proven. With model scale tests the stability of sandwich shells was analyzed against shell buckling due to axial compression and compared to tests with steel shells. Optical measurements were used to record the geometrical imperfections and to import the imperfect geometry of such shells in FE-models. Furthermore, a comparison of critical buckling loads was carried out with numerical solutions. The test series show a significant increase in bearing capacity for sandwich cylinders, which depends on the compressive strength of the core materials. The sandwich shells with a grout as core material show a catastrophic post buckling like steel shells. In contrast to this the elastomer core supports a ductile post buckling. The failure criteria for all variants of tested sandwich shells is more a local failure due to the steel faces called face wrinkling and not a global shell buckling.

KEY WORDS: hybrid tower; wind energy; shell stability; sandwich cylinder; core material; axial loading, buckling.

NOMENCLATURE

E	Young's modulus
f_{uk}	Characteristic tensile strength
f_{yk}	Characteristic yield strength
l	Length of cylinder
M	Moment
N	Axial compression force
r	Radius
t	Nominal wall thickness
u	Deformation
ε_{el} ; ε_{pl}	Elastic strain; plastic strain
κ	Buckling reduction factor
ν	Poisson's ratio in elastic range
σ	Stress

INTRODUCTION

A lot of steel constructions like substructures of offshore wind energy converters consist of cylindrical shells and tubular members. One reason for this is, that columns with a circular hollow section (CHS) have higher buckling loads compared to columns with a rectangular hollow (RHS) or a solid section (SS) for the same weight [Schmidt, 2004]. But for members with CHS the shell stability must be taken into account in the design procedure. If the stability is not sufficient different modes of shell buckling can lead to catastrophic failure of the whole steel construction. The knowledge about shell buckling increased very fast within the last decades and was included in several international standards and recommendations [EC 3 1993-1-6, 2007], [DIN 18800-4, 1990].
The intention of every engineer, planning offshore steel constructions, is to increase the bearing capacity and if possible saving weights simultaneously. With regard to axially compressed steel shells the use of high-strength steels could be one opportunity for this challenge. But the comparison in table 1 for the buckling loads of a cylindrical tower section ST S235 with steel grade S235 and a ST S460 with S460 shows that only the use of high-strength steels does not satisfy the intention.

Table 1. Comparison of buckling loads for cylindrical tower sections

Parameter	Unit	ST S235	ST S460
Young's modulus E	MPa	210000	
Length l	mm	30000	
Radius r	mm	2750	
Thickness t	mm	50	24
Yield strength f_{yk}	MPa	215	460
Ideal buckling stress $\sigma_{x,Rcr}$	MPa	1423	977
Ideal buckling load $N_{x,Rcr}$	MN	1229	407
Buckling reduction factor κ_2	-	0.87	0.59
Real buckling stress $\sigma_{x,Rk}$	MPa	187	257
Real buckling load $N_{x,Rk}$	MN	161	113

The tower section with S235 has a length of l = 30 m, radius of r = 2.75 m and a wall thickness of t = 50 mm. Because the thickness is greater than 40 mm the yield strength f_{yk} has to be reduced from 235 to 215 MPa [EN 10025-2, 2004]. For the S460 tower section the wall thickness can be decreased to 24 mm concerning the yield strength ratio 215/460 = 0.47. Therefore, the ideal buckling stresses are calculated according to [Flügge, 1962] and for the same boundary conditions (BC 2 at the bottom and top of the tower section), where the buckling reduction factor κ_2 [DIN 18800-4, 1990] has to be used for axially compressed shells. As result the real buckling load of the S460 cylinder with 107 MN is significant lower as for the S235 cylinder with 161 MN. The ratio of utilization falls from 87 % for S235 to 59 % for S460. Thus, only the use of high strength steels is not recommended for tower sections of wind energy converters without any stiffeners. But nevertheless to use the increase of strength and reduction of weight due to high strength steels a sandwich cylinder offers a new alternative solution for tower sections of offshore wind energy converters as shown in Fig. 1.

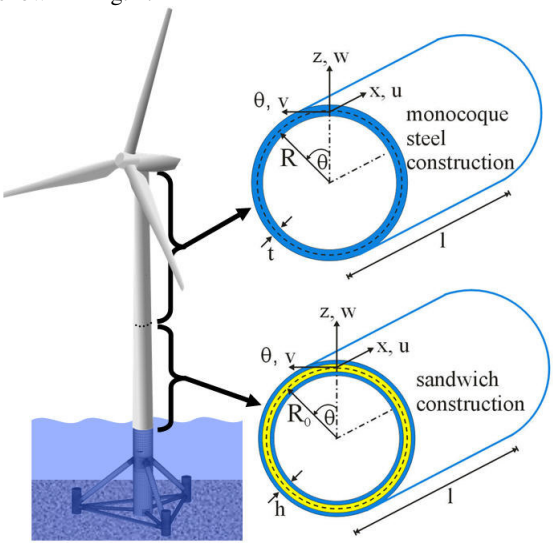

Figure 1. Hybrid tower for an offshore wind energy converter

In this paper the shell stability for a hybrid tower of an offshore wind energy converter and especially for the sandwich section is presented. The hybrid tower consists of different tubular sections, where the upper section is a monocoque steel shell construction and the lower one is a sandwich construction (s. Fig. 1). This section has two steel shells which are bonded together with a core material. Compared to a monocoque steel section the shell thickness is divided into an inner and outer steel face. The core between them increases the stability of the shells. Therefore, the use of sandwich construction, compared to monocoque construction of the same face material, produces structures with much higher overall buckling loads.
The following chapters deal with sandwich and composite shell theories which are used to estimate the stability of such double skin shell constructions. Furthermore, a model scale test series is carried out to analyze the influence of different core materials. The test specimens are loaded by uniform axial compression to observe the shell buckling. The deformations and strains are measured by optical 3D sensors to localize critical zones. The experimental results are compared to numerical simulations including measured geometrical imperfections. The FE-model is validated by a laminate composite shell theory. Within a numerical pre-design the use of high strength steels for the inner and outer face is also considered to compare the various types of tower configurations. The goal is to find the best combination of steel faces with a core material in the ultimate limit state for the hybrid tower of an offshore wind energy converter.

SHELL THEORY FOR SANDWICH CYLINDERS

Over the years a significant literature has evolved of methods of analysis and design for sandwich constructions subjected to various mechanical and environmental loads. An overview of the methods and theories is included in [Kapania, 1989] and [Vinson, 1993]. To analyze the stability of sandwich cylinders the laminate composite shell theory is used presented in [Vinson, 1993]. Therefore, effects of anisotropy and asymmetry to the mid-plane of sandwich shell cross sections can be considered.
The geometry of such sandwich cylinders is shown in Fig. 1 with the length l, the radius R_0 of the mid-plane and the thickness h. The definition for deformations (u, v, w) is based on the cylindrical coordinate system (x, θ, z). The mid-plane of the sandwich shell is used as reference surface, which is in case of symmetry the mid-plane of the core material. Thus, the core is defined as layer 0 with the thickness t_0. The nomenclatures for the other layers with thicknesses t_{-1} for the inner steel face and t_{+1} for the outer steel face are shown in Fig. 2.

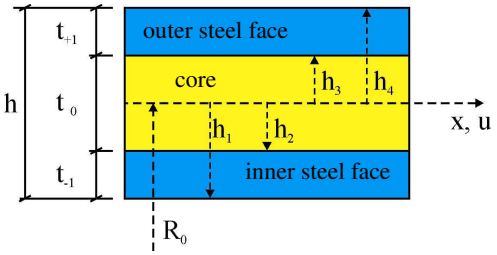

Figure 2. Cross sectional with nomenclature of a sandwich shell

The laminate composite shell theory includes the Love's hypotheses:

$$\sigma_Z = \varepsilon_Z = \varepsilon_{ZX} = \varepsilon_{Z\theta} = 0 \tag{1}$$

$$u_{tot} = u_0(x,\theta) + \beta_X(x,\theta)\cdot z \tag{2}$$

$$v_{tot} = v_0(x,\theta) + \beta_\theta(x,\theta)\cdot z \tag{3}$$

$$w = w(x,\theta) \tag{4}$$

The expressions u_0 and v_0 are the in-plane mid surface deflections at z = 0 and w is the radial deflection. The parameters β_X and β_θ are rotations in the x and θ directions, respectively, of a lineal element that was normal to shell middle surface prior loading. For an elastic material, both stress σ_{ij} and strains ε_{kl} are second order tensor quantities, where in three dimensional space they have $3^2 = 9$. They are equated by means of the fourth order elasticity tensor, C_{ijkl}, which therefore has $3^4 = 81$ components, with the resulting constitutive equation $\sigma_{ij} = C_{ijkl} \cdot \varepsilon_{kl}$. Hence by the symmetry in the stress and strain tensors the elasticity tensor immediately reduces to 36 components ($C_{ijkl} = C_{klij}$). In addition, if only orthogonally anisotropic materials are investigated the components $C_{16} = C_{26} = C_{36} = C_{45} = 0$. Therefore, the elasticity tensor for orthotropic materials is shown below:

$$C_{ij} = \begin{bmatrix} C_{11} & C_{12} & C_{13} & 0 & 0 & 0 \\ C_{21} & C_{22} & C_{23} & 0 & 0 & 0 \\ C_{31} & C_{32} & C_{33} & 0 & 0 & 0 \\ 0 & 0 & 0 & C_{44} & 0 & 0 \\ 0 & 0 & 0 & 0 & C_{55} & 0 \\ 0 & 0 & 0 & 0 & 0 & C_{66} \end{bmatrix} \tag{5}$$

So, for orthotropic elastic bodies, such as composite materials in three dimensional configuration, there are nine elasticity constants, remembering that $C_{ij} = C_{ji}$. The values for the elasticity constants can be determined depending on Young's modulus E, shear modulus G and Poisson's ratio ν as followed:

$$C_{11} = E_{11} \cdot (1 - \nu_{23}\nu_{32}) / \Delta;\ C_{22}\ and\ C_{33}\ analogous \quad (6)$$

$$C_{12} = E_{11} \cdot (\nu_{21} + \nu_{31}\nu_{23}) / \Delta;\ C_{13}\ and\ C_{23}\ analogous \quad (7)$$

$$with\ \Delta = 1 - \nu_{12}\nu_{21} - \nu_{23}\nu_{32} - \nu_{31}\nu_{13} - 2 \cdot \nu_{21}\nu_{32}\nu_{13}$$

$$C_{44} = G_{23}; \quad C_{55} = G_{13}; \quad C_{66} = G_{12} \quad (8)$$

The previous equations are the generalized constitutive formula for one lamina of a composite structure. Consider a sandwich construction composed of three or more layers the constitutive equations have to be formulated for each layer. Furthermore, the orientation of every layer is taken into account multiplying the elasticity tensor with the transformation matrix which includes terms for angles of fiber directions [Lam, 1998]. Thus, the reduced and transformed elasticity tensor for the k^{th} layer can be written as

$$\bar{C}^k = T^{-1} \cdot C^k \cdot T \quad (9)$$

The analyses of sandwich constructions as the lower tower section in Fig. 1 involves in-plane stiffness's A_{ij}, flexural stiffness's D_{ij} and should the steel faces of different thicknesses or materials also bending stretching couplings B_{ij} exist. Therefore the stiffness's can be formulated as:

$$A_{ij} = \sum_{k=1}^{n} \bar{C}_{ij}^k \cdot (h_k - h_{k-1}) \qquad with\ i, j = 1, 2, 6 \quad (10)$$

$$B_{ij} = \frac{1}{2} \sum_{k=1}^{n} \bar{C}_{ij}^k \cdot (h_k^2 - h_{k-1}^2) \qquad with\ i, j = 1, 2, 6 \quad (11)$$

$$D_{ij} = \frac{1}{3} \sum_{k=1}^{n} \bar{C}_{ij}^k \cdot (h_k^3 - h_{k-1}^3) \qquad with\ i, j = 1, 2, 6 \quad (12)$$

Finally the integrated stress-strain and moment curvature relations for the cylindrical sandwich shell are given by the following equation presented in [Vinson, 1993]:

$$\begin{bmatrix} N_X \\ N_\theta \\ N_{X\theta} \\ M_X \\ M_\theta \\ M_{X\theta} \end{bmatrix} = \begin{bmatrix} A_{11} & A_{12} & 2A_{16} & B_{11} & B_{12} & 2B_{16} \\ A_{21} & A_{22} & 2A_{26} & B_{12} & B_{22} & 2B_{26} \\ A_{16} & A_{26} & 2A_{66} & B_{16} & B_{26} & 2B_{66} \\ B_{11} & B_{12} & 2B_{16} & D_{11} & D_{12} & 2D_{16} \\ B_{12} & B_{22} & 2B_{26} & D_{12} & D_{22} & 2D_{26} \\ B_{16} & B_{26} & 2B_{66} & D_{16} & D_{26} & 2D_{66} \end{bmatrix} \cdot \begin{bmatrix} \varepsilon_X^0 \\ \varepsilon_\theta^0 \\ \varepsilon_{X\theta}^0 \\ \kappa_X^0 \\ \kappa_\theta^0 \\ \kappa_{X\theta}^0 \end{bmatrix} \quad (13)$$

The normal forces are estimated by multiplying the in-plane stiffness's A_{ij} with the strains of the reference surface (z = 0). In the case of asymmetry the influence of moments on the strains is considered by B_{ij}. Analogous B_{ij} would then establish a relationship between curvatures and normal forces. Furthermore, the moments are determined multiplying the flexural stiffness's D_{ij} with the curvatures of the finite sandwich shell element.

LINEAR BUCKLING ANALYSES

In case of buckling due to axial compression the critical buckling load is $N_x = N_{x,,cr}$ and $N_\theta = N_{x\theta} = M_x = M_\theta = M_{x\theta} = 0$. If a sandwich shell with mid-plane symmetry is investigated the components $B_{ij} = 0$. The stresses can then be compared to the allowable or failure stress in each layer. Furthermore, all layers (faces and core) should have isotropic material properties. For this special case the equation to use is:

$$N_{x,cr} = \frac{\pi^2 m^2 D_{11}}{L^2} \left(1 + 2\frac{D_{12}}{D_{11}}\beta^2 + \frac{D_{22}}{D_{11}}\beta^4 \right) + \frac{\gamma^2 L^2}{\pi^2 m^2 R_0^2} \left(\frac{A_{11}A_{22} - A_{12}^2}{A_{11} + \left(\frac{A_{11}A_{22} - A_{12}^2}{A_{66}} - 2A_{12} \right)\beta^2 + A_{22}\beta^4} \right) \quad (14)$$

where $$\beta = \frac{nL}{\pi R_0 m} \quad (15)$$

$$\gamma = 1 - 0.901\left(1 - e^{-\phi}\right) \quad (16)$$

$$\phi = \frac{1}{29.8} \left[\frac{R_0}{\sqrt[4]{\frac{D_{11}D_{22}}{A_{11}A_{22}}}} \right]^{0.5} \quad (17)$$

Here γ is an empirical (knock down) factor that insures that the calculated buckling load will be conservative with respect to all experimental data that are available [NASA SP-8007, 1968]. To determine the critical buckling load the integers m und n have to vary to determine the minimum value for $N_{x,cr}$ in MN/m. The integer m is the number of half waves in axial direction and the integer n is the number of full waves in circumferential direction.
A parameter study was carried out to check if this classical shell theory for laminate composites is also applicable for sandwich cylinders of such tower section shown in Fig. 1. For the calculations the dimensions of table 1 were used for the steel tower sections ST S235 and ST S460, which were compared with two configurations for sandwich tower sections. The first sandwich construction is a combination of steel-grout-steel (SGS), where a grout was used as core material. The second is a combination of steel-elastomer-steel (SES). In this case polyurethane with excellent bonding characteristics was taken into account for the core. The various thicknesses and the material properties are summarized in table 2.

Table 2. Parameters for the tower sections ST, SGS and SES

Type	Layer thicknesses t_{-1} / t_0 / t_{+1} in mm	Young's modulus of core E_0 in MPa	Poisson ratio ν_0
ST S235	50	-	-
ST S460	24		
SGS S235	25 / t_0 / 25	33800	0.20
SGS S460	12 / t_0 / 12		
SES S235	25 / t_0 / 25	870	0.36
SES S460	12 / t_0 / 12		

The inner and outer steel faces are considered with Young's modulus of $E_{-1} = E_{+1} = 210000$ MPa and Poisson's ratio of $\nu_{-1} = \nu_{+1} = 0.30$. As core material properties $E_0 = 33800$ MPa, $\nu_0 = 0.20$ for the grout and $E_0 = 870$ MPa, $\nu_0 = 0.36$ for the elastomer were taken into account for the parameter study. All tower sections has a length of $l = 30$ m and a mid-plane radius of $r_0 = 2.75$ m. The thickness of the steel tower sections is considered as $t_{ST} = t_{-1} + t_{+1}$ (s. Fig. 2) and for the sandwich constructions is t_{-1} the thickness for the inner steel face and t_{+1} for the outer steel face.

As result of the parameter study the buckling curves of each tower configuration are determined due to the variation of the integer's m and n in Eq. 14. For example the buckling curves of a sandwich cylinder SGS S460 with layer thicknesses $t_{-1} / t_0 / t_{+1} = 12 / 40 / 12$ mm are shown in Fig. 3. Therefore, the critical buckling stresses for various values between m = 1 and 20 are plotted depending on the number n_{wave} of full waves in circumferential direction.

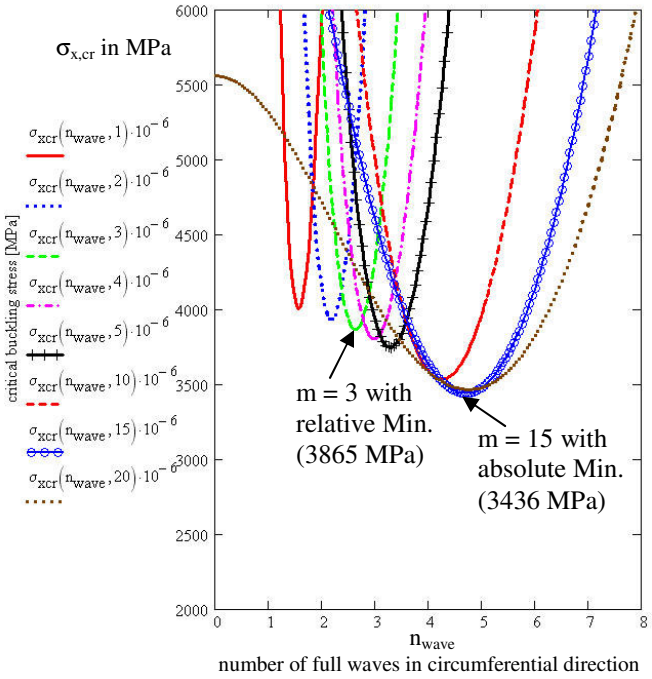

Figure 3. Buckling curves for a sandwich cylinder SGS S460

Each stress value in Fig. 3 is calculated with the following equation, where A_{-1} is the cross section of the inner steel shell and A_{+1} the cross section of the outer steel shell:

$$\sigma_{x,cr}(n_{wave}, m_{wave}) = \frac{N_{x,cr}(n_{wave}, m_{wave}) \cdot 2\pi \cdot R_0}{A_{-1} + A_{+1}} \qquad (18)$$

For each buckling curve a relative minimum of $\sigma_{x,cr}$ exist, for example the minimum value for $m_{wave} = 3$ is 3865 MPa near $n_{wave} = 3$. The comparison with a numerical simulation shows a very good agreement in Fig. 4, where the buckling mode with m = 3 half waves in axial direction, n = 3 full waves in circumferential direction and the critical buckling stress value of 3914 MPa fit very well to the laminate shell theory according to [Vinson, 1993]. In Fig. 3 the absolute minimum of $\sigma_{x,cr} = 3436$ MPa is reached for the combination $n_{wave} = 5$ and $m_{wave} = 15$. Buckling curves with $m_{wave} > 15$ have again higher relative minima as 3865 MPa. The lower border line would be like a garland, which is also known for isotropic monocoque shells.

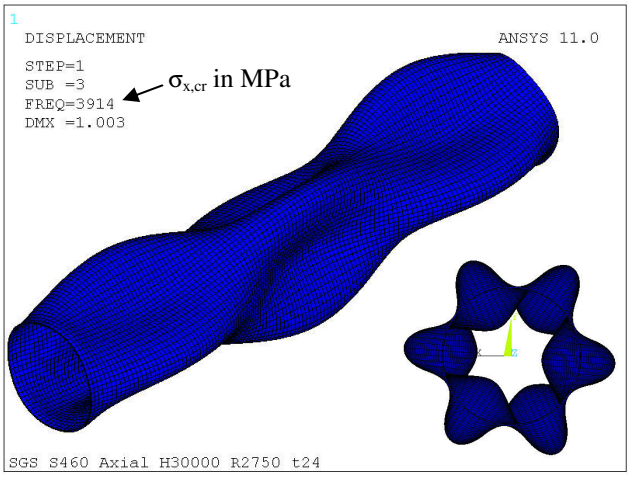

Figure 4. Buckling mode for SGS S460 with m = 3 and n = 3

All results of the parameter study are summarized in Table 3 to compare the critical buckling stresses derived from numerical simulations with values of shell theories for monocoque shells according to [Flügge, 1962] and composite shells presented in [Vinson, 1993]. The composite shell theory is also for monocoque shells applicable, but the numerical results for ST S235 and ST S460 have a better agreement to the shell theory according to Flügge.

Table 3. Comparison of critical buckling stresses

Type	Layer thicknesses $t_{-1} / t_0 / t_{+1}$ in mm	$\sigma_{x,cr}$ in MPa		
		[Flügge]	[Vinson]	FEM
ST S235	50	1423	1509	1404
ST S460	24	977	714	962
SGS S235	25 / 40 / 25	-	4722	4760
SGS S460	12 / 40 / 12	-	3865	3914
SES S235	25 / 40 / 25	-	4001	3984
SES S460	12 / 40 / 12	-	3052	2865

For the comparison between composite shell theory and FEM the same combinations for m and n have to be considered. Therefore, the results for SGS and also for SES agree very well based on the chosen configuration of face and core thicknesses. To check a wide range of core thicknesses the parameter study was expand to $t_0 = 0 – 100$ mm. Thus, the numerical and theoretical results are plotted in Fig. 5.

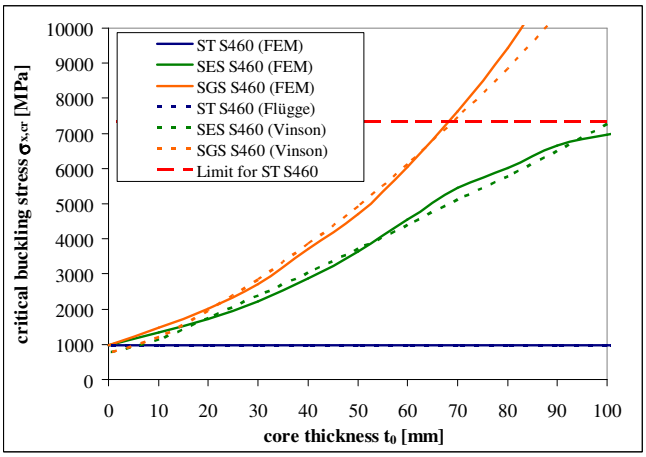

Figure 5. Comparison of critical buckling stresses for S460 depending on the core thickness

OPTIMIZATION OF A SANDWICH TOWER SECTION

The goal is to find the best combination of steel faces with a core material in the ultimate limit state for a sandwich tower section of an offshore wind energy converter. The core should be thick enough to increase the shell stability as much as possible but also thin to saving weights. However, the maximum shell stability would be reached if the yield stress has not be reduced due to a buckling reduction factor, for example if the factor κ_2 is equal 1.0 for axially compressed shells according to [DIN 18800-4, 1990]. The value $\kappa_2 = 1.0$ is valid when the shell has a non-dimensional slenderness ratio which is $\lambda_{Sx} \leq 0.25$. Thus, the optimized buckling stress values $\sigma_{x,cr,opt}$ can be determined with the following formulas:

$$\bar{\lambda}_{Sx} = \sqrt{\frac{f_{y,k}}{\sigma_{x,cr}}} = 0.25 \qquad for \qquad \kappa_2 = 1.0 \tag{19}$$

$$\sigma_{x,cr,opt} = \frac{f_{y,k}}{\bar{\lambda}_{Sx}^2} = \frac{f_{y,k}}{0.25_{Sx}^2} = 16 \cdot f_{y,k} \tag{20}$$

Therefore, a sandwich shell with steel faces of S235 has an optimized buckling stress estimated to 3760 MPa and for a sandwich shell with S460 the value is $\sigma_{x,cr,opt} = 7360$ MPa. The second value is also plotted as limit line in Fig. 5, which is crossed due to the curve for SGS S460 nearly $t_0 = 68$ mm. This is the core thickness that belongs to the optimized configuration for the sandwich tower section SGS using high strength steel faces with $t_{-1} = t_{+1} = 12$ mm. Because the SES with an elastomer core is weaker the optimized core thickness would be nearly 100 mm. Since the tower sections for offshore wind energy converters are normally designed in the elastic range it is not recommended or necessary to increase the buckling stresses and core thicknesses over the optimized values. For the sandwich tower section with S235 the optimized buckling stress (3760 MPa) is reached when $t_0 = 30$ mm for SGS S235 and $t_0 = 35$ mm for the SES S235.

With these optimized core thicknesses the steel faces can be utilize up to yield stress and no reduction due to shell buckling is necessary in the elastic range (s. Eqs. 19 and 20). A comparison for the real buckling loads in Fig. 6 shows the increase in shell stability which is possible with sandwich tower sections in contrast to monocoque steel tower sections. Herein, the real buckling loads are calculated with regard to [EC 3 1993-1-6, 2007] where the steel cylinder ST S235 is defined as reference type with 100 % buckling load.

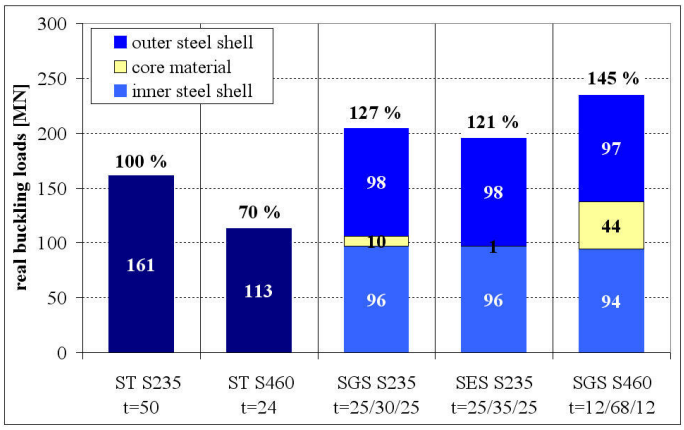

Figure 6. Increase of real buckling loads with sandwich tower sections

Due to the steel thickness of t = 50 mm the yield strength has to be reduced for the ST S235 to 215 MPa [EN 10025-2, 2004]. Since the steel thickness for SGS S235 and SES S235 is splitted in two steel faces the reduction of yield stress is only 225 MPa. For the SGS S460 and SES S460 with the optimized shell thicknesses the yield stress do not have to be reduced [EN 10137-2, 1995] which is an advantage for the sandwich construction with high strength steels.

In comparison to the reference cylinder ST S235 in Fig. 6 the ST S460 has a lower buckling load (-30 %, s. also Table 1). Thus, the ST S460 would be not economic and is cancelled as alternative solution for tower sections of offshore wind energy converters. But with sandwich tower sections a significant increase in overall buckling loads is possible. For example the buckling load of SES S235 is with 195 MN (+21 %) much higher as for the reference cylinder ST S235. The value for SGS S235 is even 204 MN which is an increase of 27 % compared to the reference type. It has to be mentioned that the buckling loads correspond to the bearing capacity in the ultimate limit state, since no reductions due the overall shell buckling are necessary. Therefore, the bearing capacities of the core materials are additionally considered for the comparison in Fig. 6. Herein, the compressive strength of the grout material is much higher as for the elastomer core the ratio of bearing capacity is higher for the SGS S235 as for the SES S235. The values are estimated in the elastic range according to [DIN 18800-5, 2005] for composite structures. But this national standard is not applicable for all structural design calculations of the sandwich construction because of the higher slenderness the cylinders can not be declared as composite column structures. However, the stress-strain relations can be used and they are valid up to the limit of elastic range which is also the design limit for substructures of wind energy converters. Furthermore, with regard to the economy the additional bearing capacity of the grout core is beneficial or even necessary to justify the extra costs for this core material.

With these assumptions a further increase would be possible with the configuration as SGS S460. In this case the steel faces can be also loaded up to the yield strength and the bearing capacity of the core material increases according to the stress strain relation and due to the higher core thickness. This type of tower section is very interesting because simultaneously to the increase in bearing capacity a reduction in overall weight is possible as shown in Fig. 7. The intention of every planning engineer to increase bearing capacities coupled with saving tonnage, as formulated in the introduction, seems to be possible with sandwich constructions for tower sections of wind energy converters.

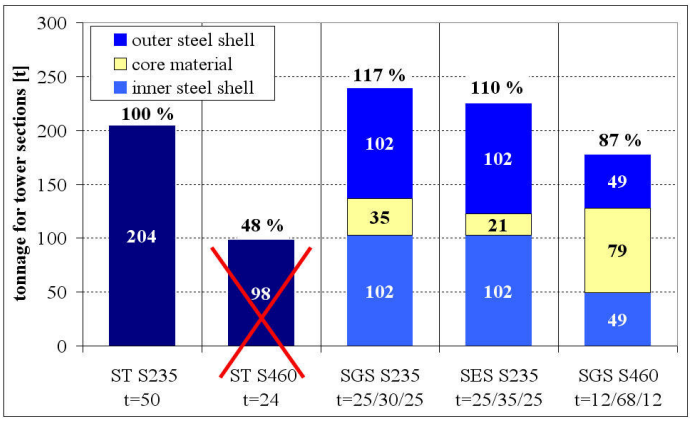

Figure 7. Comparison of tonnage between the tower sections

The comparison of tonnage in Fig. 7 is based on the following mass densities:

- Steel: $\rho_S = 7850$ kg/m³
- Grout: $\rho_G = 2280$ kg/m³
- Elastomer: $\rho_E = 1150$ kg/m³

The ST S235 with 50 mm shell thickness has been defined as reference tower section with 100 % tonnage again. The use of high strength steel leads to a reduction, the ST S460 weights only 48 %. But the buckling load of this type is to low in contrast to the reference cylinder. Thus this tower section without any stiffeners can not be recommended for an alternative design study.
The higher buckling loads for SGS S235 and SES S235 are only possible with additional tonnages due the core material. Therefore the SES S235 weights 10 % and the SGS weights 17 % more than the reference cylinder ST S235. But the use of the high strength steel S460 in combination with a grout material as core the tonnage can be decreased (-13 %). Together with the increase in buckling loads (+45 %) the SGS S460 is a more lightweight structure with great shell stability compared to the ST S235 and offers a very interesting new alternative solution for tower sections.
The optimization can also be carried out with the goal to find the best configuration with the same buckling load as the reference type (161 MN = 100 % of ST S235). In this way the optimized layer combination for SGS S460 would be $t_{-1} / t_0 / t_{+1} = 8 / 60 / 8$ mm with only 135 tonnages. The reduction in overall weight is then calculated to -34 %. The steel tonnage drops from 204 t for S235 to 65 t for S460. Considering the actual prices for the steel grades there would be enough saving in costs to cover the additional costs for the grout material.
However, in the comparison it has also to be taken into account that two cylindrical steel shells for one sandwich tower section have to manufacture which produces higher costs. Additionally the costs for the injection process of the core material have to be considered. On the other side there are saving in costs for welding possible because the volume for the seam welds decreases in square with the shell thickness. Concerning the weld details not only the ultimate limit state (ULS) of such a sandwich tower section is important but also the fatigue limit state (FLS). Therefore it is necessary to increase the fatigue strength for the steel faces and mainly for the seam welds additionally to the increase in stability against shell buckling. For example the fatigue resistance can be significant enhanced with methods of post weld treatment.
The design study above is carried out only for axially compressed tower sections, but also the other loads of an offshore wind energy converter such as bending and torque has to be taken into account. The nodding moment, the torsion and the thrust of the turbine dominate the stresses in the tower sections. Therefore the laminate shell theory presented in [Vinson, 1993] is also applicable for these loads and the buckling criteria can be estimated with the same A, B, D-matrix of Eq. 13. For example the buckling due to torsion and a comparison between the buckling loads for various monocoque and sandwich tower sections is presented in [Schaumann, 2006].
In comparison to a reinforced concrete tower section for onshore wind energy converters a sandwich tower section has the advantage that the steel faces function already as formwork shells during the production process. Furthermore, the hoping effect of the steel faces to the core material is also an advantage for the new tower concept.
In contrast to conventional composite structures where shear connectors are used the forces between the layers of a sandwich cylinder should be transferred over adhesion. This criteria that the adhesive bonding between the steel faces and the core is ensured at the whole contact area and at every time and that the full laminar stiffening remains intact in the elastic range up to yield stress of the steel faces, has been assumed for the design study above. Whether this assumption is justified was the interest of a buckling test series at the institute for steel construction of the Leibniz University Hannover. Herein, various sandwich cylinders were loaded with uniform axial compression. The experimental results of this test series are presented in the next chapters.

TEST SETUP FOR SANDWICH SHELL BUCKLING

The buckling tests with axial compression at sandwich cylinders were carried out on a 600 kN servo hydraulic testing machine. The test setup is shown in Fig. 8.

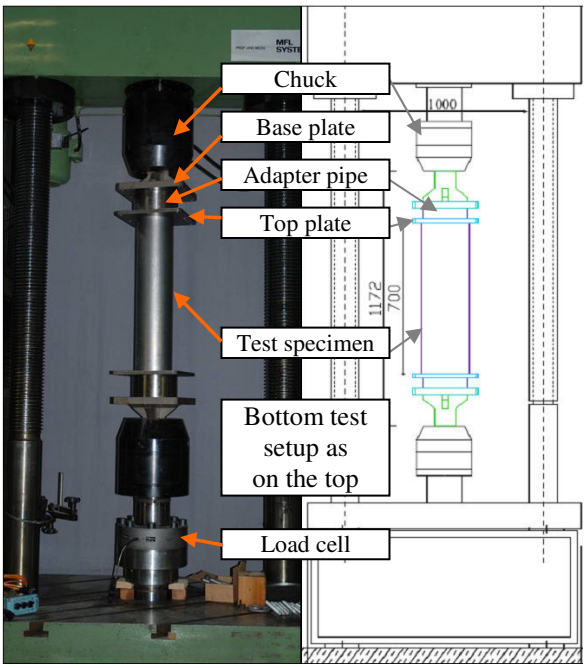

Figure 8. Test setup for buckling tests

The test specimen has a top and a bottom plate at the ends and is vertical positioned between the supporting elements. The axial force is induced over base plates and measured with a load cell. Adapter pipes were used between the base and top plates to get a uniform pressure in circumferential direction. In addition, top and bottom plate have circular slots according to the diameter of the test specimen to ensure ideal supporting conditions.

TEST SPECIMEN

As core three different injectable materials were tested. The first grout was the SikaGrout 311 from Sika Deutschland GmbH, the second one was V1/10 from Pagel Spezialbeton GmbH, both consist of mineral components. Additionally an elastomer (two-component polyurethane) from Elastogran GmbH was used as core material. The most important mechanical properties of all composite materials are listed in table 4.

Table 4. Parameter of core materials

Company	Core material	Young's modulus E	f_{ck} after 1day	f_{ck} after 28 day
		[MPa]	[MPa]	[MPa]
Sika	Grout 311	37000	28	78
Pagel	V1/10	35300	39	91
Elastogran	Elastomer	870	18	18

The values for the Young's modulus are taken from the datasheets of the companies. In contrast to both grout materials the elastomer has a significant lower value for the Young's modulus, thus the elastomer core is much weaker. The values for the compressive strength after 1 and 28 days were measured in the laboratory. After one day the grout materials have already a high early-strength. The compressive strength

of the elastomer depends on the temperature but after 1 day nearly 90 % of the final strength is reached for the composite material with excellent bonding characteristics. The high early-strength is important for injection processes in situ. Both grout materials have the mass density of 2280 kg/m³ as already used for the calculations in the parameter study. The elastomer core with a mass density of 1150 kg/m³ has an advantage with regard to the comparison of tonnage.
Since two different grout materials based on mineral components were tested, the type SGS (steel-grout-steel) gets the extensions SGS_s for Sika and SGS_p for Pagel. As steel faces the X2CrTi12 was used for inner and outer steel shells. The yield stress of this steel grade corresponds to a S235. The measured yield strength is 236 MPa and the tensile strength is 432 MPa at a strain at failure of 34 %.
The geometric data of the tested cylinders is summarized in Table 5. All test specimens has a length (height) of 700 mm. In addition to the buckling tests with sandwich cylinders the inner and outer steel shells were also used for tests with steel cylinders. Therefore, the inner steel shell with 0.7 mm was ST_1 and the outer steel shell with 0.8 mm was ST_2. These thin steel faces were chosen to get a high slenderness for elastic shell buckling. The steel cylinders ST_1 and ST_2 were also useful to check if the test setup was applicable for buckling tests.

Table 5. Geometry of test specimens

Type of cylinder	Length L	Radius R_0	Layer thicknesses t_{-1} / t_0 / t_{+1}
	[mm]	[mm]	[mm]
ST_1	700	72.55	0.7
ST_2		84.20	0.8
SGS_s		78.40	0.7 / 10.9 / 0.8
SGS_p			
SES			

The layer configuration for the sandwich cylinders is fixed due the geometry of inner and outer steel shell. Thus, the core has a thickness of 10.9 mm. The thickness ratio between the face and core is nearly 1:15 (0.75:10.9) and is doubled so high as the optimized ratio in the parameter study for the SGS S460 with 1:7.5 (8:60). It has to be mentioned that the core thickness can not be too thin for the model scale tests because the core materials must be injectable. Therefore, the maximum grain size for both grouts was 1 mm and for the elastomer core significant lower as 1 mm, which is an advantage for this composite material. The injection processes are shown in Fig. 9.

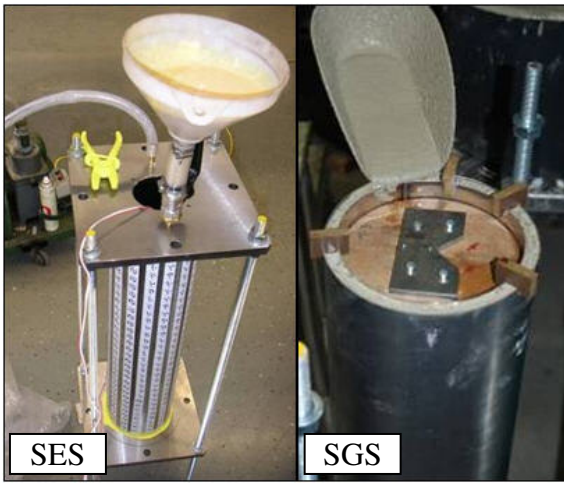

Figure 9. Injection of core materials for SES and SGS
The injection process of the elastomer was carried out with bottom and top plate to ensure a closed cavity. The elastomer was filled in with an inlet valve. At the outlet valve a vacuum pump was used to support the injection. After 10 minutes coupling processes of the two components of the elastomer began. During this exothermic reaction the elastomer expands (6 % of core volume). Due to this expansion it is ensured that the elastomer is bonded at the whole contact area to the steel faces. The maximum measured temperature was 85°C and 6 hours after injection the sandwich cylinder (SES) reached the room temperature again.
The injection of both grout materials was carried out without the top plate (s. Fig. 9). A closed cavity was in these cases not necessary. The shrinkage of the grout materials can be compensated with additive. All injection processes could be carried out without any problems. Some cuts at the sandwich cylinder after the buckling tests approved the correct bonding without any holes or leaks.
The geometrical imperfections of all cylinders were measured with 3D optical methods. Therefore, 528 coded targets were applied to the surface of the outer steel face as shown in Fig. 10. The automatic 3D-calculation of the coordinates was carried out with the optical measurement system TRITOP® and alternative with PhotoModeler6®. These systems have included various interfaces to other program packages for additional vectorial calculations like reverse engineering. As result the coded targets can be plotted in a 3D virtual space. A best-fit-analysis was carried out to estimate the maximum ovalization of each measured circular level (s. Fig. 10 right).

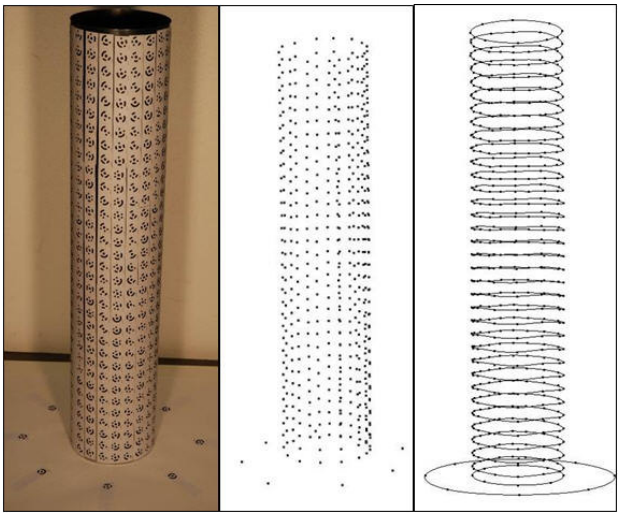
Figure 10. Optical measurements of the cylinders

The maximum depth of pre-bulges was calculated to 0.23 mm outside and to 0.03 mm inside. These measured values were under the allowable tolerance of 0.29 mm according to DIN 18800-4 for a cylinder with dimensions as ST_1. The maximum out of roundness (ovalization) was estimated to 0.35 % which is also under the 2 % limit for cylinders with $R \leq 250$ mm according to DIN 18800-4. Thus, the geometrical imperfections of the test specimen keep in the valid range of tolerance according to German recommendations for cylindrical steel shells.

RESULTS OF BUCKLING TESTS

The buckling tests were carried out after the optical measurements of geometrical imperfections for all test specimens and the injection processes. The test specimens were positioned vertically with bottom and top plate in the testing machine as shown in Fig. 8. Both sandwich cylinders with grout as core material (SGS_s and SGS_p) were tested one day after injection, thus the compressive early-strength $f_{ck} = 28$ and 39 MPa have to be considered for the test evaluation. All buckling tests

were carried out displacement controlled and with a speed of 0.008 mm/s. During the tests the strains were measured using strain gauges attached to the outer surface of the cylinders. The displacements in axial direction were recorded online by inductive sensors. The applied axial force was measured with a load cell. In addition the ARAMIS® system was used for optical 3D deformation measurements. It is ideally suited to measure, with high temporal and local resolution three-dimensional deformations and strains of a chosen surface and not only punctual as with strain gauges. For the static loaded cylinders, ARAMIS® was used for a non-contact and material independent determination of 3D coordinates, 3D displacements, strain tensors and strain rates. Thus, the development of shell buckling during the tests could be recorded in a new quality.
First of all, the steel cylinders ST_1 and ST_2 were tested as reference cylinders to check if the test setup is suitable for shell buckling. For example the optical measured deformations are shown in Fig. 11 and compared to a photo of ST_1. The buckle started near the bottom plate and the form is similar to the elephant foot buckling mode which is well known from literature.

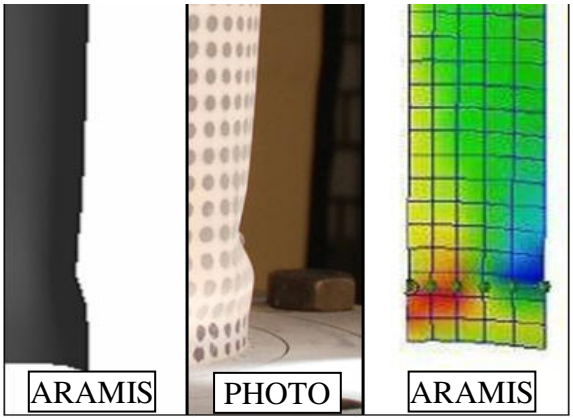

Figure 11. Measuring of buckling deformations at ST_1

All test results of shell buckling are summarized in Fig. 12 as load-displacement-curves. The axial force could be increased for the sandwich cylinders. The buckling loads of all sandwich test specimens were over the limit of elasticity of the steel faces which is estimated to 178 kN (N_{pl,ST_1} = 75 kN from inner steel face and N_{pl,ST_2} = 103 kN from outer steel face). The buckling loads of SGS_p and SGS_s are very high (356 and 306 kN). The higher value for SGS_p can be explained with the higher early-strength of the Pagel Grout V1/10 compared to the Sika Grout 311 in table 4.

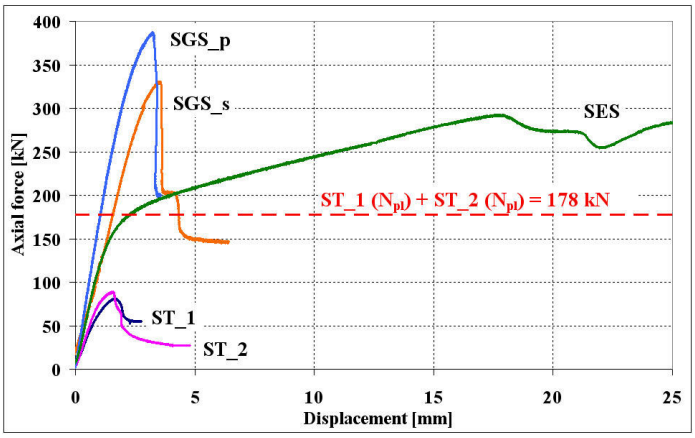

Figure 12. Buckling tests with steel and sandwich cylinders

These test results attest that the grout materials participate at the bearing capacity as known from composite columns. For both sandwich variants with grout the same post buckling behavior can be observed as the steel variants. The sudden drop (collapse) in bearing capacity is typical for buckling modes of shells under axial compression. But in contrast to this the SES with an elastomer core has a very good post buckling behavior – no significant reduction in bearing capacity appeared. The axial force could be increased up to 293 kN by a displacement of 18 mm. This kind of stability based mainly on the excellent bonding characteristics of the elastomer which could also transfer the forces between the layers in the plastic range of the steel shells. Furthermore, it can be recognized that the nonlinearity of the SES-curve started near 180 kN which corresponded approximately to the limit of elasticity of the steel faces. This can be explained with the lower stiffness and the lower compressive strength of the elastomer core. It is weaker compared to the cores with grout materials.
The comparison of all buckling loads is presented as κ-factors in table 6. On the one hand as ratio between experimentally estimated axial load N_{exp} and plastic axial force of both steel shells $N_{pl,ST}$ and on the other hand as ration between N_{exp} and total plastic axial force $N_{pl,tot}$ including the strength of the core materials.

Table 6. Comparison of all buckling loads

Type of cylinder	N_{exp} [kN]	$N_{pl,tot}$ ($N_{pl,ST}$) [kN]	$\kappa = N_{exp} / N_{pl,tot}$ ($N_{exp} / N_{pl,ST}$)
ST_1	81	75 (75)	1.08 (1.08)
ST_2	89	103 (103)	0.86 (0.86)
SGS_s	330	306 (178)	1.08 (1.85)
SGS_p	387	356 (178)	1.09 (2.17)
SES	293	275 (178)	1.07 (1.65)

The ST_1 buckled in the plastic range (κ = 1.08) but the ST_2 collapsed due to elastic shell buckling (κ = 0.86). The increase of the κ-factor for the sandwich cylinders (165 %, 185 % and 217 %) corresponded to the sequence of compressive strength values for the core materials (s. Table 4). The higher the compressive strength the higher the buckling loads of the sandwich construction. If the participation of the core on the bearing capacity is considered the κ-factor is still over the value of 1.0. Thus the steel faces must be stressed over the yield stress. That was the goal of the parameter study at the beginning where the shell stability should be increased so far to avoid elastic shell buckling. The stability of sandwich shells can be mainly optimized with the thickness, the Young's modulus and the compressive strength of the core material. Since elastic shell buckling could be avoided other failure modes occurred in the plastic range of the sandwich cylinders for example face wrinkling as shown in Fig. 13.

Figure 13. Face wrinkling of a sandwich cylinder (SGS)

Face wrinkling can occur in a sandwich construction either when subjected to a compressive buckling or in the compressive face during bending. A wrinkle that becomes unstable causes an indentation in the core if the compressive strength of the core is lower than the tensile strength. The second mode of face wrinkling is possible if the wrinkle causes a gap between the core and the faces if the tensile strength of the core is lower than the compressive strength. Whichever case applies, a poor adhesive core will undoubtedly reduce the allowable wrinkling stress of the sandwich. After buckling tests the top plate of the SGS_s was opened and additionally a longitudinal cut was done to check the cross section and the bonding between the layers. In Fig. 13 it can be recognized that the second mode of face wrinkling occurred where the wrinkle cause a gap between the core and the steel faces. Outside of the area of face wrinkling the bonding was intact for all tested sandwich cylinders.
As result the shell stability of sandwich constructions could be ensured up to the limit of elasticity with sufficient bonding behaviors for all tested core materials. The increase in buckling loads was very high and the steel faces could be stressed over the yield strength. Furthermore, the additional bearing capacity due to the core materials in the elastic range offered a further increase in buckling loads compared to monocoque steel constructions.

NUMERICAL BUCKLING ANALYSES

In addition to the buckling tests numerical simulations were carried out to analyze the sandwich shell buckling modes and to compare it with test results. In contrast to typical geometrically and materially nonlinear buckling analysis with included imperfections (GMNIA) these numerical simulations were executed with measured real geometrical imperfections. Therefore, the 3D-coordinates of the optical measured shell structures as shown in Fig. 10 were imported by an interface to the FE-program ANSYS®. The nonlinear material properties of the steel faces were considered with true stress-strain relations estimated by tensile tests. The steel cylinders were modeled and meshed with SHELL93-elements and two types of layered elements were chosen for the sandwich constructions, at first SHELL91-elements and second SOLSH190-elements. The last one is used for simulating composite shell structures with a wide range of thickness. All element-types have features like plasticity, hyperelasticity, stress stiffening, large deflection and large strain capabilities, which are necessary for the investigated applications. For example the load-displacement-curves were compared for the SES in Fig. 14.

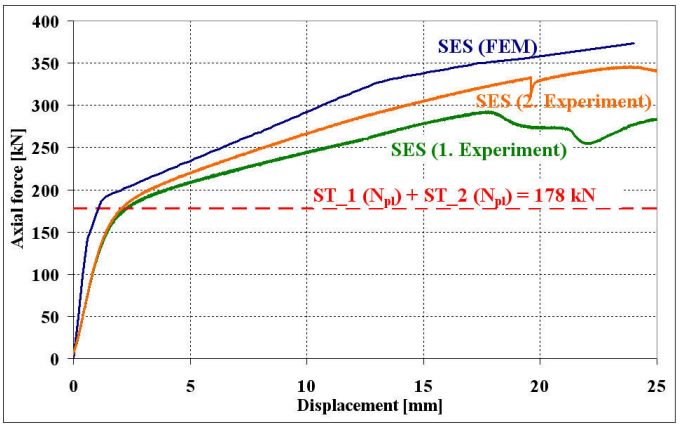

Figure 14. Comparison of load-displacement-curves for SES

The curve estimated numerically is more stiffener in the elastic range as both tested SES-cylinder. The difference can be explained with additional deformations of the test setup. Especially the delayed deformations in the ring slots of the top plates were also recorded of the test machine as total displacement. In contrast the FE-model is modeled without the test setup and top plates (s. Fig. 4), thus only the effective displacement of the test specimen is calculated. However, the qualitative run of the curves agree very well. The begin of nonlinearity is at the same load level (180 kN) and also the slope in the plastic range corresponds to the test results. The FE-model must be extended with contact elements to simulate interface delamination as face wrinkling where a gap between the layers can be occurred. Therefore, the values have to be determined for maximum allowable tensile contact pressure and the maximum friction stress of the core materials.
Finally a comparison between theory, experiment and simulation was carried out for all steel and sandwich cylinders. For the steel shells the experimentally estimated buckling loads were over the minimum values of the German recommendation [DIN 18800-4, 1990] which were chosen as theoretical results. The numerical results calculated with GMNIA-buckling analyses including real geometrical imperfections have a good agreement with the test results (s. Fig. 15).

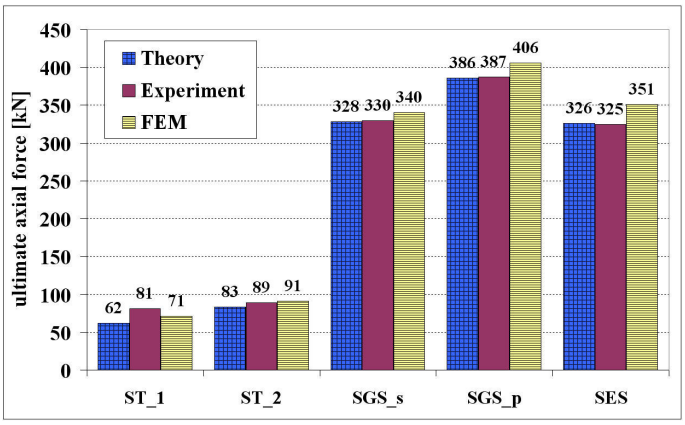

Figure 15. Comparison of ultimate axial force for all tested cylinders

As theoretical values for the sandwich variants the axial force at the strain of failure was chosen. Therefore, the proportionate axial forces of each layer were determined with the following equation based on the measured stress-strain-relations.

$$N_{theory} = A_{-1} \cdot \sigma_{-1}(\varepsilon) + A_0 \cdot \sigma_0(\varepsilon) + A_{+1} \cdot \sigma_{+1}(\varepsilon) \qquad (21)$$

The calculation of the theoretical results for SGS and SES in Fig. 15 is summarized in table 7. The values for N_{theory} agree very well to the measured axial loads (N_{exp}) compared for the point (displacement, strain) at failure.

Table 7. Bearing capacity of sandwich variants

Parameter	SGS_s	SGS_p	SES
$A_{-1}/A_0/A_{+1}$ [mm²]	365 / 5369 / 370		
u at failure [mm]	3.6	3.3	18.0
ε at failure [%]	0.51	0.47	2.57
$\sigma_{-1}/\sigma_0/\sigma_{+1}$ [MPa]	242/28/242	241/39/241	313/18/313
$N_{-1}/N_0/N_{+1}$ [kN]	88/150/90	88/209/89	114/96/116
N_{theory} [kN]	328	386	326
N_{exp} [kN]	330	387	(293) 325

The comparison shows that the consideration of additional bearing capacities due to the core materials is valid which offers a good performance concerning the sandwich shell stability of tower sections.

CONCLUSIONS

Alternatively to a steel tower section for wind energy converters a sandwich tower section was analyzed with regard to the stability. At first a comparison between cylindrical shells with steel grade S235 and S460 showed that the shell with S460 has a lower buckling load if the reduction in thickness was considered according to the ratio of yield stresses. Thus, a steel tower section with S460 would be not economic without any stiffeners and is not recommended as alternative solution for tower sections of offshore wind energy converters. But with sandwich tower sections in combination with high-strength steels a significant increase in overall buckling loads would be possible.
The sandwich shell consisted of an inner and outer steel face, which were bonded adhesively to different core materials between them. Two grout and one elastomer core were investigated in this parameter study. In comparison with linear buckling analyses the validity of a laminate composites shell theory was proven. The results showed a good agreement between shell theory and numerical simulations where a significant increase in shell stability for sandwich cylinders was estimated. Therefore, the inner and outer steel faces could be loaded up to the yield stress considering an optimized core thickness. In this case the core materials operated as full laminar stiffening and produced an increase of critical buckling stresses. The shell stability can be optimized with the Young's modulus of the core material and additionally to the variation of core thickness. The goal was to find the best combination of steel faces with a core material in the ultimate limit state for sandwich tower sections of wind energy converters. Due to the reached plastic buckling loads the combination of high-strength steels is in principle possible to get tower sections which will be optimized with regard to stability and weight. The design study was carried out only for axially compressed tower sections, but also the other loads of an offshore wind energy converter such as bending and torque has to be taken into account.
The theoretical investigations of sandwich shell buckling were continued with buckling tests to check the bonding characteristics and ultimate bearing capacities. Within this test series sandwich cylinders were analyzed against shell buckling due to axial compression and compared to tests with monocoque steel cylinders. It could be successfully checked with these steel shells that the test setup was suitable for shell buckling tests. The test series showed a significant increase in bearing capacity for the sandwich cylinders, which also depends on the compressive strength of the core materials. The sandwich shells with a grout show a catastrophic post buckling as known from steel shells. In contrast to this the elastomer core supports a ductile post buckling. The failure criteria for all variants of tested sandwich shells is more a local failure due to face wrinkling in the plastic range and not due to a overall shell buckling. As result the shell stability of sandwich constructions could be ensured up to the limit of elasticity with sufficient bonding behaviors for all tested core materials. The series of tests shall be continued with sandwich cylinders in combination with high-strength steels using as steel faces.
Furthermore, optical measurements were used to record the geometrical imperfections and to import the imperfect geometry of such shells in FE-models. Thus, a comparison of critical buckling loads could be done with numerical simulations based on geometrically and materially nonlinear buckling analysis with included imperfections. The results have a good agreement to the experimental results.
Finally a comparison between theory, experiment and simulation was carried out for all steel and sandwich cylinders. The comparison showed that the consideration of additional bearing capacities due to the core materials was valid and in combination with high-strength steels it could be offered a new alternative solution for tower sections of offshore wind energy converters.

ACKNOWLEDGEMENTS

The authors would like to thank the German companies Brugg Rohrsysteme GmbH, Elastogran GmbH, Pagel Spezialbeton GmbH as well as Sika Deutschland GmbH for the test specimen and core materials. Further thanks should also be given to SIAG AG which manufactured the test setup. In addition the authors would like to acknowledge for the financial support of the project GROW (grout structures for offshore wind energy converters) provided by the German Federal Ministry for the Environment, Nature Conversation and Nuclear Safety. The authors are also grateful to the Institute of Building Materials and Institute of Materials Science of the Leibniz University Hannover for material tests on the steel and core materials.

REFERENCES

DASt-Guideline 013 (1980). "Beulsicherheitsnachweise für Schalen, Deutscher Ausschuss für Stahlbau", Stahlbauverlag.

DIN 18800-4 (1990). "Stahlbauten - Stabilitätsfälle, Schalenbeulen" *NABau im DIN e.V.,* Beuth-Verlag.

DIN 18800-5 (1990). " Verbundtragwerke aus Stahl und Beton - Bemessung und Konstruktion " *NABau im DIN e.V.,* Beuth-Verlag.

DIN EN 1993-1-6 (2007). "Bemessung und Konstruktion von Stahlbauten – Teil 1-6: Festigkeit und Stabilität von Schalen", *Eurocode 3*, Beuth Verlag.

EN 10025-2 (2004). "Warmgewalzte Erzeugnisse aus Baustählen", *Techn. Lieferbedingungen für unlegierte Baustähle*, CEN.

EN 10137-2 (1995). "Blech und Breitflachstahl aus Baustählen mit höherer Streckgrenze im vergüteten oder im ausscheidungsgehärteten Zustand", *Techn. Lieferbedingungen für vergütete Stähle*, CEN.

Helfers, B (2007). "Bemessung und Simulation hybrider Turmkonstruktionen für Windenergieanlagen", *Master thesis*, Institute for Steel Construction, Leibniz University Hannover.

Kapania, RK (1989). "A review on the analysis of laminated shells" *J. Pressure Vessel Technology*, Vol. 111, pp 88-96.

Knorr, HM (2007). "Experimentelle und numerische Untersuchungen zur Schalenstabilität von Sandwichzylindern", *Diploma thesis*, Institute for Steel Construction, Leibniz University Hannover.

Lam, KY, and Loy, CT (1998). "Influence of boundary conditions for a thin laminated rotating cylindrical shell" *Elsevier Composite Structures*, Vol. 41, pp 215-228.

Schaumann, P, Keindorf, C, Matuschek, J and Stihl, T (2006). "Schalenbeulen von Sandwichzylindern mit einem neuen Elastomer als Verbundwerkstoff" *Stahlbau*, Vol. 75, No 9, pp 748-753.

Schmidt, H (2004). "Schalenbeulen im Stahlbau" *Essener Unikate*, Vol. 23, pp 71-85.

Stamm, K, and Witte, H (1974). "Sandwichkonstruktionen" *Ingenieurbauten*, Vol. 3, Springer-Verlag.

Vinson, JR (1993). "The behavior of shells composed of isotropic and composite materials" University of Delaware, USA, Kluwer Academic Publishers.

Zenkert, D (1997). "An introduction to sandwich construction" Warley, West Midlands, Engineering Materials Advisory Services, Ltd.